Accepted Manuscript

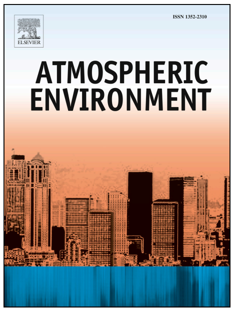

Improving satellite aerosol optical Depth-$PM_{2.5}$ correlations using land use regression with microscale geographic predictors in a high-density urban context

Yuan Shi, Hung Chak Ho, Yong Xu, Edward Ng

PII: S1352-2310(18)30468-0

DOI: 10.1016/j.atmosenv.2018.07.021

Reference: AEA 16127

To appear in: *Atmospheric Environment*

Received Date: 1 February 2018

Revised Date: 6 July 2018

Accepted Date: 9 July 2018

Please cite this article as: Shi, Y., Ho, H.C., Xu, Y., Ng, E., Improving satellite aerosol optical Depth-$PM_{2.5}$ correlations using land use regression with microscale geographic predictors in a high-density urban context, *Atmospheric Environment* (2018), doi: 10.1016/j.atmosenv.2018.07.021.

Improving Satellite Aerosol Optical Depth-$PM_{2.5}$ Correlations Using Land Use Regression with Microscale Geographic Predictors in a High-density Urban Context

Yuan Shi[*, a], Hung Chak Ho [b,c], Yong Xu [d], and Edward Ng [a, e, f]*

[a] School of Architecture, The Chinese University of Hong Kong, Shatin, NT, Hong Kong SAR, China

[b] Department of Land Surveying and Geo-Informatics, The Hong Kong Polytechnic University, Hung Hom, Hong Kong

[c] Research Institute for Sustainable Urban Development, The Hong Kong Polytechnic University, Hung Hom, Hong Kong

[d] Lyles School of Civil Engineering, Purdue University, 550 W Stadium Ave, West Lafayette, IN 47907, USA

[e] Institute of Future Cities (IOFC), The Chinese University of Hong Kong, Shatin, N.T., Hong Kong S.A.R., China

[f] The Institute of Environment, Energy and Sustainability (IEES), The Chinese University of Hong Kong, Shatin, NT, Hong Kong SAR, China

*The Corresponding Author:

Postal address: Room 505, AIT Building, School of Architecture, The Chinese University of Hong Kong, Shatin, NT, Hong Kong SAR, China

Phone: +852 3943 9428

Email address: shiyuan@cuhk.edu.hk (Secondary email: shiyuan.arch.cuhk@gmail.com)

Abstract

Estimating the spatiotemporal variability of ground-level $PM_{2.5}$ is essential to urban air quality management and human exposure assessments. However, it is difficult in a high-density and highly heterogeneous urban context as ground-level monitoring stations are most likely sparsely distributed. Satellite-derived Aerosol Optical Depth (AOD) observation has made it possible to overcome such difficulty due to its advantage of spatial coverage. In this study, we improve the AOD-$PM_{2.5}$ correlations by combining land use regression (LUR) modelling and incorporating microscale geographic predictors and atmospheric sounding indices in Hong Kong. The spatiotemporal variations of ground-level $PM_{2.5}$ over Hong Kong were estimated using MODerate resolution Imaging Spectroradiometer (MODIS) AOD remote sensing images for the period of 2003-2015. An extensive LUR variable database containing 294 variables was adopted to develop AOD-LUR models by seasons. Compared to the baseline models (fixed effect models include only basic weather parameters), the prediction performance of all annual and seasonal AOD-LUR fixed effect models were significantly enhanced with approximately 20-30% increases in the model adjusted R^2. On top of that, a mixed effect model covers time-dependent random effects and a group of geographically and temporally weighted regression (GTWR) models were also developed to further improve the model performance. As the results, compared to the uncalibrated AOD-$PM_{2.5}$ spatiotemporal correlation (adjusted R^2 = 0.07, annual fixed effect AOD-only model), the calibrated AOD-$PM_{2.5}$ correlation (the GTWR piecewise model) has a significantly improved model fitting adjusted R^2 of 0.72 (LOOCV adjusted R^2 of 0.65) and thus becomes a ready reference for spatiotemporal $PM_{2.5}$ estimation.

Keywords

land use regression; aerosol optical depth; $PM_{2.5}$; spatial mapping

Graphical Abstract

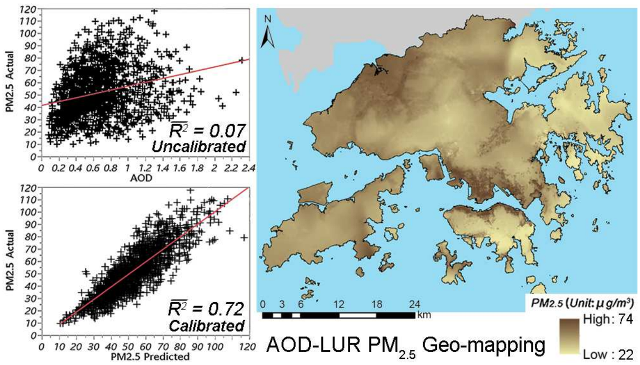

Highlight

- AOD-$PM_{2.5}$ spatiotemporal correlation of Hong Kong was investigated;
- Land use regression (LUR) method was adopted to improve the AOD-$PM_{2.5}$ correlation;
- Microscale geographic variables and sounding indices were incorporated as predictors;
- MLR, LME and GTWR models were developed for the daily estimation of $PM_{2.5}$;
- The improved AOD-$PM_{2.5}$ correlation - GTWR model has an adjusted R^2 of 0.72.

1. INTRODUCTION

Ambient particular matter (PM) is a mixture of extremely small solid particles and liquid droplets, which contains complex components of nitrates and sulfates, organic chemicals, metals, and dust particles (EPA, 2013). $PM_{2.5}$ (fine particulate matter with < 2.5 microns in aerodynamic diameter) has been identified as a great threat to population health (Davidson et al., 2005; Dockery, 2009; Schwarze et al., 2006), and thus the observations of spatiotemporal variability of $PM_{2.5}$ has become one of the most important topics in epidemiology (Pope et al., 1995) and urban climatology (Bach, 1972). The strong associations between long-term or short-term health risks and ambient $PM_{2.5}$ exposure were not only be found in the typical urban form in cities in North America or Europe, but also in cities with compact and high-density built environment such as Hong Kong (Lin et al., 2017; Tam et al., 2015; Wong et al., 1999; Wong et al., 2002). $PM_{2.5}$ is also responsible for various negative effects on the living environment, such as urban climate deterioration (Jonsson et al., 2004) and visibility reduction (Cheung et al., 2005; Thach et al., 2010; Wu et al., 2005). Moreover, these adverse effects are expected to be stronger in a high-density environment because of the poor wind ventilation (Yuan et al., 2014). Therefore, estimating the spatiotemporal variation of $PM_{2.5}$ is essential to air quality management and health risk assessment.

Although a prediction of spatiotemporal variability of $PM_{2.5}$ across a city is necessary, it is generally difficult because of the sparse distributions of air monitoring stations (Kanaroglou et al., 2005), especially in a high-density city. For example, hourly $PM_{2.5}$ concentration in Hong Kong is currently monitored by a local air quality monitoring network (AQMN) with only 16 stations. However, Hong Kong is a large city with approximately 1,100 km^2 of land covering with a wide range of urban settings (in terms of topography, land use, building form and residents’ activities, etc.). This diversity means air quality varies greatly across districts, and cannot be effectively monitored by the ground-level monitoring network with sparsely distributed stations (Shi et al., 2016). This consequently leads to the probable issue of assessment errors in the investigation of human exposure when using the $PM_{2.5}$ data from the nearest monitoring station. Moreover, identifying hotspots of human exposure will be difficult when only AQMN is used.

Alternatively, satellite-based aerosol optical depth (AOD) data with large spatial coverage and temporal continuity have been popularly used to estimate ground-level $PM_{2.5}$ concentration in global and regional contexts (Hoff and Christopher, 2009). Previous studies have observed a fair correlation between $PM_{2.5}$ measured by AOD and local air monitoring networks (Krstic and Henderson, 2015; Paciorek et al., 2008), and found the ability of predicting the spatial distribution of $PM_{2.5}$ by AOD and chemical transportation models (Geng et al., 2015; Liu et al., 2004; van Donkelaar et al., 2006). Some studies also suggested that applying AOD with advanced statistical methods such as machine learning and spatial statistical models may be able to improve the spatial quality of $PM_{2.5}$ mapping (Beckerman et al., 2013). Most of these studies have focused on the spatial distribution of $PM_{2.5}$ in a relatively large geographic extent with homogeneous landscapes (Qin et al., 2017; Zang et al., 2017). Only a few cases incorporated the microscale environmental factors to AOD-$PM_{2.5}$ modelling (Kloog et al., 2012). Actually, it is more essential in a high-density built environment, because the microscale effect on the spatial accuracy of $PM_{2.5}$ prediction is significantly affected by the urban morphology. Due to this limitation, only a few AOD-$PM_{2.5}$ studies have incorporated with microscale environmental factors in a fine spatial resolution mapping. For example, the study with $PM_{2.5}$ prediction map in 100m-resolution was an application to traditional European cities with relatively homogenous landscape (de Hoogh et al., 2016), while the other studies are of 500m resolution or even coarser that are not suitable for representing the spatial variability of $PM_{2.5}$ in an extremely heterogeneous urban area. Moreover, the heterogeneous land surface also affects the vertical distribution of aerosol, which is also a major impact factor in the AOD-$PM_{2.5}$ relationship that should be taken into consideration (Li et al., 2015).

To overcome the above limitations, several studies have attempted to enhance the AOD-$PM_{2.5}$ correlations by combining Land Use Regression (LUR) modelling with microscale land use information and geographic predictors (Kloog et al., 2012; Lee et al., 2016; Mao et al., 2012; Vienneau et al., 2013). LUR is a promising technique for estimating spatial variation of ambient air pollution at a fine scale. It has been widely adopted in human pollution exposure assessments in public health studies (Hoek et al., 2008; Ryan and LeMasters, 2007). Using geographic and urban setting predictors, LUR allows the estimation of long-term averaged concentration of ambient air pollution in unmonitored areas in geographic information system (GIS). Attempts to develop temporal-resolved LUR models have been made in recent years (Saraswat et al., 2013). These estimations will provide a series of fine-scale maps of spatially and temporally varying ground-level $PM_{2.5}$ at a finer spatial resolution compared to the satellite AOD data.

The aim of this study is to improve the AOD-$PM_{2.5}$ correlation analysis and to provide a better estimation of the spatiotemporal variation of ground-level $PM_{2.5}$ in a city with high-density built environment, in order to fill the monitoring gaps of the local monitoring network. Hong Kong has been selected as the study site, because it is a high-density city with distinct urban form across districts. The spatial variation of urban characteristics across both natural and artificial surfaces can considerably modify the boundary layer meteorological conditions, and subsequently affect the aerosol vertical distribution. Ultimately, the spatial variation of ground-level $PM_{2.5}$ is affected by non-uniformly distributed local sources and the variation of urban forms at the microscale. In this study, we enhance the spatiotemporal AOD-$PM_{2.5}$ correlation analysis for Hong Kong by combining LUR modelling with a comprehensive set of microscale geographic predictors as well as atmospheric sounding indices. Fine-scale spatiotemporal variation of ground-level $PM_{2.5}$ over Hong Kong is estimated using LUR with the MODerate resolution Imaging Spectroradiometer (MODIS) AOD data for the period of 2003-2015.

2. MATERIALS AND METHODS

2.1 GROUND-LEVEL $PM_{2.5}$ LONG-TERM MONITORING DATA

In this study, hourly concentration of ground-level $PM_{2.5}$ between 2003 and 2015 were obtained from 15 of 16 stations operated under the AQMN of Hong Kong Environmental Protection Department (EPD), because a newly-constructed station in Tseung Kwan O are not available for the entire study period. (Figure 1). These hourly $PM_{2.5}$ concentration monitored by the AQMN are based on high-accuracy gravimetric sampling using the USEPA certified gravimetric oscillating microbalance equipment, including the Graseby Anderson PM, Partisol 2025, R&P TEOM series 1400-AB and 1405DF (Lu and Wang, 2008). Daily average of $PM_{2.5}$ concentration was calculated in order to be consistent with the AOD data for further analysis (Figure S-1 in the supplementary materials).

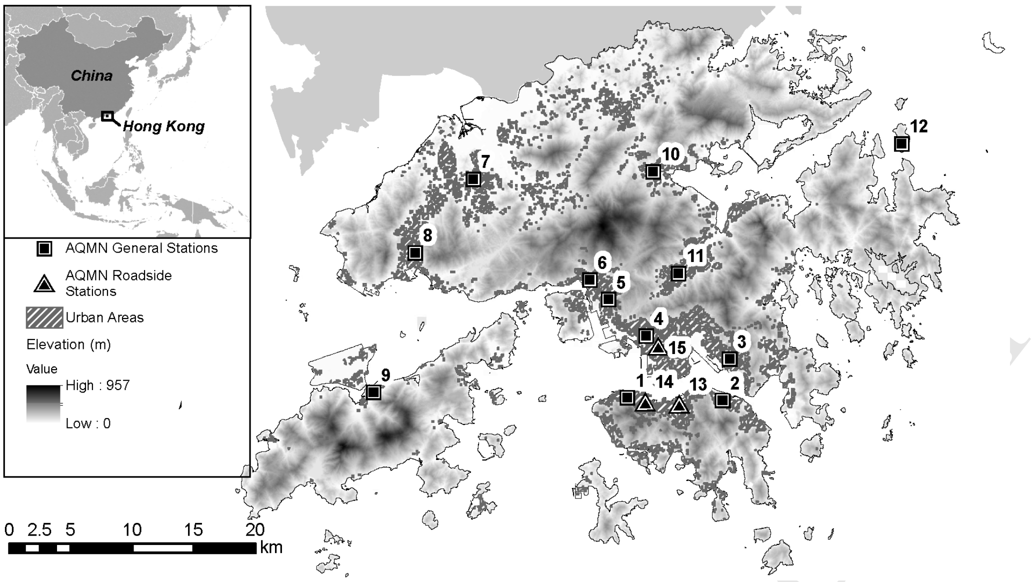

Figure 1. The locations of 15 available stations in the air quality monitoring network (AQMN) of Hong Kong (The elevation of each station can be found from: http://www.aqhi.gov.hk/en/monitoring-network/air-quality-monitoring-stations.html).

2.2 AEROSOL OPTICAL DEPTH (AOD) DATA

The MODIS Level 2 aerosol products at a spatial resolution of 3 km were obtained from both Terra and Aqua satellites (MOD04_3K at 10:30 and MYD04_3K at 13:30) using dark target algorithm (Remer et al., 2013). Compared with the original 10-km product, this product with 3-km resolution is better at providing details of fine-scale aerosol characteristics over the small geographic extent with heterogeneous landscapes. There is finer resolution AOD data for worldwide, but it is not specially designed for subtropical area. Therefore, it needs to be carefully pre-calibrated (the aerosol retrieval algorithm needs to be modified) before using the data in subtropical area (Bilal et al., 2013). Therefore, we acquired the 3 km AOD product from 2003 to 2015. A total of 8,738 AOD images were obtained for the 13-year period from Terra and Aqua sensors. All AOD images were projected to the Hong Kong 1980 coordinate system for the spatial consistency of local land use data sets. Daily averaged AOD values were calculated based on above satellite images at grid cells corresponding to the 15 AQMN stations. Satellite AOD observations are not available when clouds cover the location. All available observations from the entire AOD image data set were extracted (Figure S-2 in the supplementary materials).

2.3 METEOROLOGICAL VARIABLES

Weather data (ground-level air temperature, relative humidity, wind speed, rainfall, mean sea level pressure, wet-bulb temperature and dew-point temperature) were retrieved from a total of 42 weather stations of Hong Kong Observatory (HKO). Weather data from the closest weather stations were assigned to the grid cell locations of 15 air quality monitoring stations in AQMN. Crumeyrolle et al. (2014) mentioned that the variability in atmospheric factors such as vertical structure/mixing and hygroscopicity could significantly affect and add uncertainty to AOD-$PM_{2.5}$ correlation. Their study shows that considering the impact of ambient relative humidity could improve the $PM_{2.5}$ estimates. Moreover, the presence of aerosol above the boundary layer introduces significant uncertainties in $PM_{2.5}$ estimates. The day-to-day variation of atmospheric stability also affects the vertical distribution of aerosol (Lee et al., 2011). In that case, sounding data would serve as better predictors than the basic weather parameters. Therefore, 19 widely used sounding indices related to atmospheric stability were also adopted as meteorological variables (Table 1). The atmospheric sounding indices data used in the present study (Hong Kong, Station No. 45004) is provided by the Department of Atmospheric Science, University of Wyoming, which represent an overall atmospheric condition over entire Hong Kong for each day.

2.4 GEOGRAPHIC PREDICTORS OF PM2.5 IN LUR MODELLING

Six categories of data sets were adopted as geographic predictors of $PM_{2.5}$ LUR modelling: (i) land use, (ii) road traffic density, (iii) emission sources of marine and power stations, (iv) population density, (v) natural geography and (vi) urban surface form. Most of the geographic predictors were retrieved from the GIS vector dataset that can be accurately converted to 1m resolution for spatial study. These data have been widely and successfully used for fine-resolution mapping in Hong Kong (Shi et al., 2017). In this study, to balance the data size and mapping precision, a spatial resolution of 10m was adopted for the spatial mapping, which is also the spatial resolution of the standard land use dataset of Hong Kong. Incorporating the fine-resolution microscale geographic predictors into the estimation of AOD-$PM_{2.5}$ correlation is essentially also a data-intensive spatial downscaling process.

2.4.1 LAND USE

The limited land resources and high population jointly spawn the extremely compact urban development. The vertically developed urban form shapes the intensive and highly mixed urban land use in Hong Kong. The land use data were obtained from Hong Kong Planning Department (PlanD). The land use of Hong Kong is recorded in the raster format with a spatial resolution of 10m. Based on literature [15], the complicated land use types were reclassified as the following types: Residential use (RES); Commercial use (COM); Industrial use (IND); Government use (GOV) and Open space (OPN). Using buffering analysis, the total area (unit: m^2) of each land use type in a set of buffers (Table 1) of each monitoring stations was summed up and used as the explanatory variables of LUR modelling.

2.4.2 ROAD TRAFFIC DENSITY

Four different indicators were used to depict the local road traffic density: road line density per unit area (km/km^2), road area ratio, traffic volume counted based on passenger car unit (PCUs) and count of bus stops. Using LUR buffering analysis, line densities of five road types— expressways/trunk road, primary road, secondary road, tertiary road and ordinary road— were calculated separately. The road area ratio is the percentage of vehicle road area within a certain locality, which measures the amount of road traffic carrying capacity. The raw data of traffic flow count in Hong Kong are published in “Annual Traffic Census” by the Transport Department every year. The number of vehicles is counted at nearly 900 stations in different road segments. Based on these data and the road network, the spatial distribution of traffic volume of public transport vehicles and private/government vehicles can be mapped. Buses are heavy-duty diesel fuel vehicles and a major source of $PM_{2.5}$ in Hong Kong.(Wang and Lu, 2006) Therefore, the number of bus stops within certain buffer ranges was also used as predictors of road traffic density.

2.4.3 EMISSION SOURCES OF MARINE AND POWER STATIONS

Marine transportation accounts for a large proportion of $PM_{2.5}$ emissions in Hong Kong (Lau et al., 2007). Marine facilities and routes were identified in and extracted using GIS as point and line $PM_{2.5}$ emission sources. Local power stations relying on fossil and diesel fuels are considered area emission sources. The nearest distance from each monitoring station to the marine facilities, routes and local power plants was calculated as the predictor variables.

2.4.4 POPULATION

The population density (people per km^2) is the most commonly used measure of population distribution. The latest population census data of year 2011 is obtained from Hong Kong Census and Statistics Department and mapped using the digital boundary of Street Block/Village Clusters (SB/VC, a standard planning unit used in Hong Kong). The population density in the buffers of each monitoring stations is then calculated.

2.4.5 NATURAL GEOGRAPHY

Seven indicators were adopted as predictor variables to reflect the natural geographic condition of each monitoring station: longitude (Δx to the coordinate origin of HK1980 Gird), latitude (Δy to the coordinate origin of HK1980 Gird), elevation above the Hong Kong

Principal Datum, distance to waterfront, distance to city parks, distance to country parks and greening coverage ratio (the percentage of vegetation coverage, extracted from land use data).

2.4.6 URBAN SURFACE FORM

Densely built urban forms significantly change the aerodynamic properties of land surface, and hence change the air flow near the ground surface, resulting in considerable microscale variation in $PM_{2.5}$ concentration (Fernando et al., 2001). It has been proved that incorporating urban forms as predictor variables improves the LUR modelling accuracy (Shi et al., 2016; Tang et al., 2013). Therefore, to consider microscale environmental variations that affect the spatial accuracy of $PM_{2.5}$ prediction in a high-density city, a set of predictor variables of urban surface forms were used in LUR modelling (Barnes et al., 2014; Cao and Lin, 2014). They were building height (h), plan area index (λ_P), weighted frontal area index based on the probability of wind directions ($\bar{\lambda}_F$), urban surface roughness length (z_0), and were calculated based on the local building data set with the following equations:

$$\lambda_P = \left(\sum\nolimits_{i=1}^{n} A_{Pi}\right)/A_T \qquad \textit{Equation 1}$$

$$\bar{\lambda}_F = \sum_{\theta=1}^{16} \left[\left(\sum\nolimits_{i=1}^{n} A_{Fi(\theta)}\right)/A_T\right] P_{(\theta)} \qquad \textit{Equation 2}$$

$$z_0 = \{h - h \cdot \lambda_P{}^{0.6}\} exp\left[-\frac{K}{\sqrt{0.5 \cdot C_{Dh} \cdot \bar{\lambda}_F}}\right] \qquad \textit{Equation 3}$$

where n is the total amount of buildings in a district. A_T is the district area. A_{Pi} is the footprint area of the building i. $A_{Fi(\theta)}$ is the frontal area of building i under the scenario of wind direction θ. C_{Dh} is drag coefficient considered as 0.8. K is the Kármán's constant of 0.4. Figure 2 illustrates the mapping of spatial distribution of $\bar{\lambda}_F$ because it is not a traditional LUR predictor.

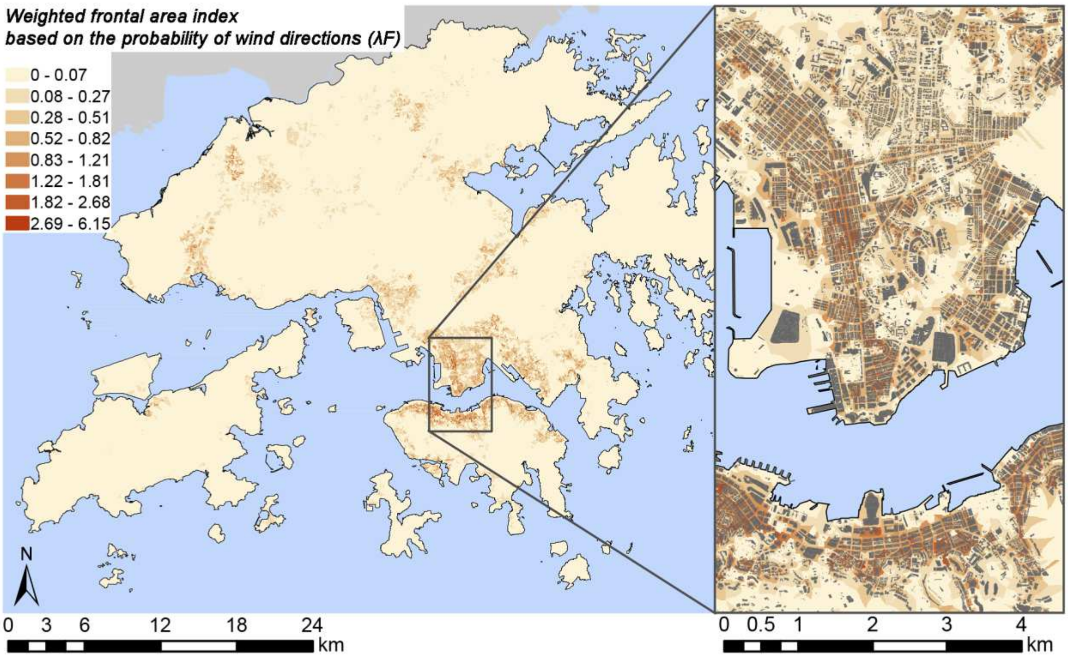

Figure 2. The spatial distribution map of weighted frontal area index based on the probability of wind directions ($\bar{\lambda}_F$) which reflects the potential of ground-level air flow movement.

261 **Table 1.** Summary of meteorological and geographic predictor variables.

Data categories	Variables	Unit	Analysis	Codes
	Meteorological variables			
Weather parameters	ground-level air temperature	*°C*	daily average	$Temp$
	relative humidity	*%*	daily average	RH
	wind speed	*m/s*	daily average	Spd
	rainfall	*mm*	daily average	Rf
	mean sea level pressure	*hPa*	daily average	*MSLP*
	wet-bulb temperature	*°C*	daily average	*Wet*
	dew-point temperature	*°C*	daily average	*Dew*
Atmospheric sounding indices	Bulk Richardson Number	-	daily average	*BRCH*
	Bulk Richardson Number using CAPV	-	daily average	*BRCV*
	Convective Available Potential Energy	*J/kg*	daily average	*CAPE*
	CAPE using virtual temperature	*J/kg*	daily average	*CAPV*
	Convective Inhibition	*J/kg*	daily average	*CINS*
	CINS using virtual temperature	*J/kg*	daily average	*CINV*
	Cross totals index	-	daily average	*CTOT*
	K index	-	daily average	*KINX*
	Pressure of the Lifted Condensation Level	*hPa*	daily average	*LCLP*
	Temperature of the Lifted Condensation Level	*K*	daily average	*LCLT*
	Lifted index	-	daily average	*LIFT*
	LIFT computed using virtual temperature	-	daily average	*LIFV*
	Mean mixed layer mixing ratio	*g/kg*	daily average	*MLMR*
	Mean mixed layer potential temperature	*K*	daily average	*MLPT*
	Total precipitable water	*mm*	daily average	*PWAT*
	Showalter index	-	daily average	*SHOW*
	SWEAT index	-	daily average	*SWET*
	Total totals index	-	daily average	*TTOT*
	Vertical totals index	-	daily average	*VTOT*
	Geographic Predictors			
Land use (Total land area within certain buffer sizes *)	Residential use	m^2	buffer	*RES*
	Commercial use	m^2	buffer	*COM*
	Industrial use	m^2	buffer	*IND*
	Government use	m^2	buffer	*GOV*
	Open space	m^2	buffer	*OPN*
Road Traffic density	Road line density of expressways/trunk road	km/km^2	buffer	*Rdexp*
	Road line density of primary road	km/km^2	buffer	*Rdpri*
	Road line density of secondary road	km/km^2	buffer	*Rdsec*
	Road line density of tertiary road	km/km^2	buffer	*Rdter*
	Road line density of ordinary road	km/km^2	buffer	*Rdord*
	Road area ratio	*%*	buffer	*Rdar*
	Traffic volume of public transport vehicles	*PCUs*	buffer	*ptpcu*
	Traffic volume of private/government vehicles	*PCUs*	buffer	*pgpcu*
	Number of bus stops	-	buffer	*busst*
Emission sources of marine & power stations	Distance to marine routes, facilities	*m*	point	*d_marine*
	Distance to local power plants	*m*	point	*d_power*
Population	Population density	$People/km^2$	buffer	*pop*
Natural geography	Longitude (based on HK1980 system)	*m*	point	*x*
	Latitude (based on HK1980 system)	*m*	point	*y*
	Elevation of the monitoring station	*m*	point	*z*
	Distance to waterfront	*m*	point	*d_water*
	Distance to city parks	*m*	point	*d_cityp*
	Distance to country parks	*m*	point	*d_countryp*
	Greening coverage ratio	*%*	buffer	*greening*
Urban surface form	building height	*m*	buffer	*h_bldg*
	plan area index	*%*	buffer	λ_P
	weighted frontal area index based on the probability of wind directions	-	buffer	$\bar{\lambda}_F$
	urban surface roughness length	*m*	buffer	z_0

The 13 buffer sizes used in this study are 50, 100, 200, 300, 400, 500, 750, 1000, 1500, 2000, 3000, 4000, 5000m.
The Sounding data available at http://weather.uwyo.edu/upperair/sounding.html

2.5 STATISTICAL MODELING AND VALIDATION METHODS

LUR modelling was conducted to develop the AOD-$PM_{2.5}$ correlation models. The $PM_{2.5}$ data mentioned in section 2.1 were used as the response variable of the models with the satellite-derived AOD mentioned in section 2.2 forced as the first explanatory variable of all regression models. The LUR modelling aims to improve the AOD-$PM_{2.5}$ correlation by incorporating microscale geographic predictors and atmospheric stability sounding indices. First, Multiple Linear Regression (MLR) method — commonly used in previous LUR studies — was adopted to identify the important predictor variables and develop traditional fixed effect model. On top of that, a mixed effect model covers time-dependent random effects and a geographically and temporally weighted regression (GTWR) model were also developed to further improve the model performance. Four steps were involved in the modelling process.

2.5.1 STEP 1 - DEVELOPING BASELINE AOD-PM2.5 MODEL

In Step 1, the baseline models of the AOD-$PM_{2.5}$ correlation were developed. The modelling only involves five most commonly used basic weather parameters mentioned in section 2.3— ground-level air temperature ($Temp$), relative humidity (RH), wind speed (Spd), rainfall (Rf) and mean sea level pressure ($MSLP$). The baseline estimation model structure in this study was forced to be built as follows:

$$PM_{2.5ij} = \alpha_1 AOD_{ij} + \alpha_2 Temp_{ij} + \alpha_3 RH_{ij} + \alpha_4 Spd_{ij} + \alpha_5 Rf_{ij} + \alpha_6 MLSP + \beta_{ij} + \varepsilon_{ij} \qquad \textit{Equation 4}$$

where $PM_{2.5ij}$ is the predicted $PM_{2.5}$ concentration at the location of air quality monitoring station i on day j. AOD_{ij} is the satellite-derived AOD at the location i on day j. α_1 is the slope of AOD. α_2, α_3, α_4, α_5 and α_6 are the slopes for the five daily averaged basic weather variables. β_{ij} is the intercept of the model. ε_{ij} is the residuals which presumably vary by day. The winter monsoon is predominant from fall to spring, making coastal Hong Kong basically downwind of the polluted industrial areas and urbanized areas in Pearl River Delta (PRD) region (Ding et al., 2013; Kok et al., 1997; Wang et al., 2009). Hence, the influence of pollution originating in densely built neighboring city of Shenzhen—north of Hong Kong—is significant. Therefore, in order to distinguish seasonal variation, the AOD-$PM_{2.5}$ correlations were developed separately using MLR by different seasons defined as annual (January to December), spring (March to April), summer (May to September), fall (October to November) and winter (December to the February of the next year). The above definitions are based on local meteorological observations and the synoptic weather pattern. Hong Kong is a coastal subtropical city influenced by monsoon. The months of each season are different than the temperate city in Europe and North America. A piecewise annual model was also developed by simply combining the four single seasonal models based on the time period of seasons. To be more specific, the piecewise model predicts the $PM_{2.5}$ in each season by separately using the four seasonal MLR correlation models in the time intervals of the four different seasons. As a result, six baseline models were developed.

2.5.2 STEP 2 - SELECTING INFLUENTIAL MODEL VARIABLES

Most of the geospatial studies treat all spatial factors using a grid system with fixed spatial resolution. However, the impact range of different influencing factors may vary due to the differences in the pollution emission intensity or the complex physical basis of the pollution diffusion and dispersion. For example, the industrial land use could affect the air quality within a spatial extent of several kilometers, while a segment of urban tertiary road will only significantly affect the air quality within a couple of hundred meters. Therefore, LUR studies apply the concept of buffers, instead of using a fixed grid system for all data. In LUR study, each air pollution influencing factor are calculated in multiple buffers. Thus, the same influencing factor calculated using two different buffer sizes are used as two separate predictor variables in the regression modelling. In this study, LUR buffering analyses were conducted for 20 geographic predictors using 13 buffer sizes. Together with other variables, 294 explanatory variables were required to be checked for developing improved the AOD-$PM_{2.5}$ correlations. In that case, it is essential to pre-select only a limited number of variables for the regression modelling because this could prevent over-fitting issues during the automatic stepwise regression modeling process (Babyak, 2004). Using the 13 buffer sizes, a series of regression analysis was performed for each buffer-based variable. The purpose of these regression analyses was to test the sensitivity of the variables in the models to different buffer sizes. These regression analyses were performed using the below model structure:

$$PM_{2.5ij} = \alpha_1 AOD_{ij} + \alpha_2 Temp_{ij} + \alpha_3 RH_{ij} + \alpha_4 Spd_{ij} + \alpha_5 Rf_{ij} + \alpha_6 MLSP + \alpha_7 VAR_d + \beta_{ij} + \varepsilon_{ij} \qquad \textit{Equation 5}$$

The model was developed for each buffer-based variable at 13 different buffers. α_7 is the slopes for the test variable (VAR_d) calculated the using buffer size of d. For example, the road traffic density calculated in 200m buffer and 2000m buffer are used as two separate variables. As described, d = 50, 100, 200, 300, 400, 500, 750, 1000, 1500, 2000, 3000, 4000, 5000m. Adjusted R^2 ($\overline{R^2}$) was used as the indicator to compare model performance. Thus, there will be 13 $\overline{R^2}$ for traffic density in the 13 buffers. By following the "A Distance Decay REgression Selection Strategy (ADDRESS)" developed by Su et al. (2009a), a distance-decay curve can be plotted, which is essentially a function of distance, and thus the critical buffers (shown as turning points/peaks in the decay curve function) could be identified. In another application study of "ADDRESS", Su et al. (2009b) detailly illustrate the identification of critical buffers. In the present study, by following the same method, only variables at the critical buffers were identified and retained as candidate explanatory variables for next step analysis.

2.5.3 STEP 3 - STEPWISE REGRESSION MODELLING

Following the typical LUR research (Beelen et al., 2013), stepwise MLR modelling was performed to develop AOD-LUR models by different seasons. The models were initially determined by using the modelling criteria of minimum Bayesian Information Criterion (BIC) using the forward direction, the model with the highest $\overline{R^2}$ was selected for further process. In the subsequent process, the p-value and variance inflation factor (VIF) of each explanatory variable in all these resultant models were examined in order to eliminate collinearity issues in the resultant models. Based on the criteria used in literature (Vienneau et al., 2013), variables with p-value > 0.10 and VIF > 5 were excluded. Due to the above criteria of variable exclusion, some of those aforementioned basic weather variables may not be included in the final models, as they naturally correlate with sounding indices (which are possibly better predictors of atmospheric stability) and are consequently removed. The final models are constructed in a general model structure as below:

$$PM_{2.5ij} = \alpha_1 AOD_{ij} + \alpha_2 VAR_{2ij} + \cdots + \alpha_m VAR_{mij} + \alpha_{m+1} VAR_{d,m+1} + \alpha_{m+2} VAR_{d,m+2} + \cdots + \alpha_n VAR_{d,n} + \beta_{ij} + \varepsilon_{ij} \quad \textit{Equation 6}$$

where $PM_{2.5ij}$ is the predicted $PM_{2.5}$ concentration at the location of air quality monitoring station i on day j. AOD_{ij} is the satellite-derived AOD at the location i on day j. α_1 is the slope of AOD_{ij}. $\alpha_2 \ldots \alpha_m$ are the slopes for the m temporally varied meteorological variables. $\alpha_{m+1} \ldots \alpha_n$ are the slopes for the $n - m$ geographic predictors (VAR_d) calculated the at the buffer size of d. β_{ij} is the intercept of the AOD-LUR model. ε_{ij} is the residuals. As a result, a total of six pairs of models (Baseline MLR vs. AOD-LUR MLR) were developed.

2.5.4 STEP 4 – INCORPORATING TIME-DEPENDENT RANDOM EFFECTS AND GEOGRAPHICAL NON-STATIONARITY

A set of traditional LUR models have been developed for Hong Kong during the first three steps. However, as mentioned earlier, traditional LUR models are commonly developed based on a fixed effect model structure, in which the effects of predictor variables are presumed to be temporally fixed. However, the influence of many predictors could be temporally variant, especially in the synoptic pattern of Hong Kong in which there are significant seasonal differences. Under such background, the influence of many predictors could be presumably at least varying by seasons. The above implies that the AOD-LUR model performance could be further improved by incorporating time-dependent effects and geographical non-stationarity into the model development. In this study, linear mixed-effect (LME) models are developed by additionally including time-dependent variables as random effects to improve the performance of AOD-LUR models. Considering the significant seasonal synoptic differences in Hong Kong (as mentioned in section 2.5.1), a categorical dummy variable was introduced to describe the seasons when particular concentration data were monitored. This newly included dummy variable is modelled in the linear regression as the random effect, such that LME models could be developed with time-dependent effects. As the results, three LME models will be developed: AOD-only LME model, baseline AOD-$PM_{2.5}$ LME model (a forced model structure with the five most commonly used basic weather parameters involved), AOD-LUR LME model (a model includes the same variable selection with the AOD-LUR stepwise MLR model). No seasonal LME models will be developed because the seasonal non-stationarity has been included in the year-round annual model. The LME model structure in this study can be expressed as:

$$PM_{2.5ij} = \alpha_1 AOD_{ij} + \alpha_2 VAR_{2ij} + \cdots + \alpha_m VAR_{mij} + \alpha_{m+1} VAR_{d,m+1} + \alpha_{m+2} VAR_{d,m+2} + \cdots + \alpha_n VAR_{d,n} + \alpha_{season,j} VAR_{season,j} + \beta_{ij} + \varepsilon_{ij} \qquad \textit{Equation 7}$$

where $PM_{2.5ij}$ is the predicted $PM_{2.5}$ concentration at the location of air quality monitoring station *i* on day *j* and the random effect variable - $VAR_{season,j}$ is added into the model structure. $\alpha_{season,j}$ is the slope of the season variable value (which presumably vary by seasons) on on day *j*. No seasonal LME models will be developed because the seasonal non-stationarity has been included in the year-round annual model. As the results, three LME models will be developed: AOD-only LME model, baseline AOD-$PM_{2.5}$ LME model (a forced model structure with the five most commonly used basic weather parameters involved), AOD-LUR LME model (a model includes the same variable selection with the AOD-LUR stepwise MLR model). No seasonal LME models will be developed because the seasonal non-stationarity has been included in the year-round annual model.

The context of land surface in the study area is highly heterogeneous which implies that the AOD-$PM_{2.5}$ correlation could also be spatially variant. Geographically weighted regression (GWR) is a commonly-used method of dealing with such spatial non-stationarity in $PM_{2.5}$ spatial estimation (van Donkelaar et al., 2015). GWR handles the spatial non-stationarity by constructing local regression for different geographical locations instead of using one linear regression for the entire study area (Brunsdon et al., 1998). However, in many cases, the regression coefficients do not remain fixed over space as well as time. To also take temporal variation into consideration, a method named GTWR has been developed for modeling spatiotemporal variation in geographical data (Huang et al., 2010) and recently adopted in ground-level $PM_{2.5}$ estimation (Bai et al., 2016). The GTWR model structure in this study can be expressed as:

$$PM_{2.5ij} = \alpha_1 AOD_{ij} + \sum_m \alpha_m(u_i, v_i, j)VAR_{mij} + \sum_n \alpha_n(u_i, v_i, j)VAR_{d,n} + \beta_{ij} + \varepsilon_{ij} \quad \textit{Equation 8}$$

where $PM_{2.5ij}$ is the predicted $PM_{2.5}$ concentration at the location of air quality monitoring station *i* on day j. AOD_{ij} is the satellite-derived AOD at the location *i* on day j. u_i, v_i are the geographical coordinates of station i. α_1 is the slope of AOD_{ij}. α_m are the slopes for the m temporally varied meteorological variables VAR_{mij}. α_n are the slopes for the n geographic predictors (VAR_d) calculated the using the buffer size of d. β_{ij} and ε_{ij} are the intercept and residuals of GTWR model. More technical details can be referred to Huang et al. (2010)'s article.

2.5.5 MODEL VALIDATION

Root-mean-square error (RMSE) and $\overline{R^2}$ were calculated for both the assessment of model fit and the cross validation of resultant models. $\overline{R^2}$ and RMSE calculated as follows:

$$\overline{R^2} = 1 - (1 - R^2)\left(\frac{n-1}{n-p-1}\right) \quad \textit{Equation 9}$$

$$RMSE = \sqrt{\frac{1}{n}\sum_{i=1}^{n}\left(PM'_{2.5i} - PM_{2.5i}\right)^2} \quad \textit{Equation 10}$$

Where $R^2$is the coefficient of determination of regression models. n is the total number of data points. p is the total number of model predictor variables. $PM_{2.5i}$ is the measured value of the $PM_{2.5}$ concentration. $PM'_{2.5i}$ is the estimated $PM_{2.5}$ concentration from the resultant models. For the model validation, leave-one-out cross-validation (LOOCV) was used to validate all resultant models. Under LOOCV, all data will be split into two parts, a single data point is used for the validation data and the remaining data points used as the training dataset. This procedure is repeated n-times. There is no randomness in the split of the data into test and training sample. Therefore, performing LOOCV repeatedly always yields the same results.

3. RESULTS

All resultant models developed in this study is based on the 13-year long-term dataset. There are data limitations provided by the EPD. $PM_{2.5}$ of Hong Kong was a relatively new measurement of EPD. Each monitoring station has different start-up date for monitoring $PM_{2.5}$. The cloud coverage is also a major impact factor of the availability of the AOD data of Hong Kong. Therefore, in the present study, the all 13-year long-term monitoring data were used for the model development to minimize this data bias. As the results, the annual model will be able to predict a daily spatial $PM_{2.5}$ concentration for any day during 2003 – 2015 period, while the seasonal models will be able to provide a daily estimation for any day in the particular season during 2003 – 2015 (for example, a summer model predicts the daily spatial $PM_{2.5}$ for any summer day during 2003-2015). Considering the resultant spatiotemporal models on a daily basis, the annual or seasonal average could be easily achieved by averaging a series of daily estimations.

3.1 THE BASELINE MODELS OF AOD-$PM_{2.5}$ CORRELATION

Using the forced model structure (Step 1), a group of baseline MLR models was developed. AOD-only fixed effect model and LME model were also developed as a reference for the model performance comparison. All these resultant baseline models are listed in Table 2. Although the performance is better than AOD-only fixed effect model, results show that both the baseline MLR models and the AOD-only LME model perform relatively poor in predicting spatiotemporal ground-level $PM_{2.5}$ without incorporating the microscale geographic variables and sounding data as predictors. The summer, fall, and winter baseline MLR models and the AOD-only LME model share a similar prediction performance level of the $\overline{R^2}$ of 0.3-0.4. The Annual baseline MLR model only has a prediction performance of $\overline{R^2}$ of 0.2 while the spring baseline MLR model has the lowest $\overline{R^2}$ of less than 0.1.

3.2 THE RESULTANT AOD-LUR MODELS WITH MICROSCALE GEOGRAPHIC PREDICTORS AND SOUNDING INDICES

Corresponding to the aforementioned baseline models, a group of AOD-LUR MLR models was developed to improve the AOD-$PM_{2.5}$ correlations (Step 2-3). Based on the model variables of corresponding MLR models, an AOD-LUR MLE model and a group of AOD-LUR GTWR models were also developed to further improve the prediction performance (Step 4). All above resultant AOD-LUR models are listed in Table 2 (details of the MLR and GTWR models have been included in supplementary materials, Table S1-S7). The annual MLR model performs poorer than the seasonal MLR models naturally because of the lack of consideration on the seasonal variation. Developing GTWR models significantly improve the performance by to incorporate time-dependent effects and geographical non-stationarity into the model development. It can be seen that the resultant seasonal MLR models with geographic predictors and sounding variables perform much better than the corresponding baseline models (see actual by predict plot in Figure 3 and Figure S-3). The summer, fall, and winter AOD-LUR MLR models have a prediction performance level of the $\overline{R^2}$ of 0.5-0.6 which are moderately good. After identifying the important variables, the development of GTWR models further improve the prediction performance to a higher level of the $\overline{R^2}$ of 0.6-0.8. The actual by predicted plot shows that some data points in spring have an extremely high monitored concentration level that cannot be well predicted. A possible cause of these outliers is the impact of the severe dust storm episodes at a much larger geographical extent during spring time in Hong Kong (Lee et al., 2010). Although there are conspicuous outliers in the spring AOD-LUR model, the regression performance is significantly increased when compared with the spring baseline model ($\overline{R^2}$ from 0.07 to 0.35). As described earlier, a piecewise annual model was also developed by combining the four single seasonal models. By separately using the four seasonal MLR correlation models in the time intervals of the four different seasons, the piecewise annual model achieves a better prediction performance ($\overline{R^2}$ of 0.55) than the single MLR annual model ($\overline{R^2}$ of 0.33). As the results, a 48% increase of 0.48 in $\overline{R^2}$ of the calibrated correlation was achieved by combining AOD-$PM_{2.5}$ correlation with LUR modelling and incorporating geographic variables and sounding indices as predictors. Although the AOD-$PM_{2.5}$ correlation has been significantly increased, the model performance is still lower than some previous studies in the other regions of China. It is reasonable because those studies of China are usually focusing on a larger spatial extent with fewer concerns of change in microscale environment. For example, the previous studies by You et al. (2016) and Xie et al. (2015) . Moreover, the monitoring stations they used are mostly located in homogeneous rural settings. Above the reasons why the variation between data are relatively low, resulting in a better $\overline{R^2}$. Our study focuses on inner-city microscale variability that can be influenced by multiple geographic factors across a city, which is more difficult to predict. Similar study for exposure modelling across a city (e.g. heat exposure) also has relatively low R^2 because of this reason (Ho et al., 2014).

Table 2. List of resultant baseline models by seasons with forced model structure and improved AOD-LUR (MLR, LME and GTWR) models with geographic variables and atmospheric sounding indices as model predictors. Piecewise MLR and GTWR models are not shown in this table because they are combinations of four single-season models. About the variable name, for example, *Rdexp0500* represents the road line density of expressways/trunk road calculated within the buffer of 500m.

		Models	**Model performance evaluation**					
Model type	**Model by seasons**	**Model structure (included variables & coefficients)**	R^2	$\overline{R^2}$	**Model fitting-RMSE**	**LOOCV-RMSE**	**LOOCV-$\overline{R^2}$**	**p-value**
AOD-only fixed effect model	Annual	15.616*AOD+41.723	0.072	0.071	18.707	19.249	0.069	<0.0001*
Baseline MLR models (weather parameters-only) (regardless of p-value and VIF of meteorological variables, no other LUR variables, Table S-1)	Annual	21.030*AOD-0.802*Temp-0.463*RH-1.761*Spd-9.285*Rf-0.091*MSLP+184.058	0.199	0.196	18.875	19.070	0.194	<0.0001*
	Spring	9.294*AOD-0.840*Temp-0.077*RH-1.465*Spd-35.261*Rf+0.190*MSLP-129.230	0.096	0.070	14.410	15.761	0.064	0.0018*
	Summer	20.958*AOD+0.028*Temp-1.071*RH-1.691*Spd-0.406*Rf-0.387*MSLP+496.565	0.341	0.319	15.181	16.361	0.296	<0.0001*
	Fall	26.609*AOD+1.222*Temp-0.672*RH-2.336*Spd-89.186*Rf-0.124*MSLP+187.013	0.389	0.373	14.111	14.953	0.352	<0.0001*
	Winter	48.645*AOD+0.319*Temp-0.376*RH-0.941*Spd-184.146*Rf-0.216*MSLP+274.619	0.381	0.373	15.894	16.332	0.363	<0.0001*
AOD-LUR MLR models (with all included variables meet the criteria of p-value < 0.10 and VIF < 5, Table S-2)	Annual	24.522*AOD-0.550*Spd+25.347*$\bar{\lambda}_F$0050-(2.178e-5)*RES0400+0.358*CTOT-0.105*LCLP-0.737*PWAT+138.640	0.326	0.322	17.097	17.589	0.313	<0.0001*
	Spring	16.745*AOD-0.487*z+3.724*Rdsec2000+0.451*CTOT-1.014*PWAT+57.171	0.371	0.353	12.270	14.155	0.306	<0.0001*
	Summer	24.628*AOD+1.382*Wet+38.007*$\bar{\lambda}_F$0100-(3.538e-4)*pop0050-0.248*LCLP-0.315*PWAT-2.763*VTOT+274.492	0.605	0.589	12.761	13.163	0.571	<0.0001*
	Fall	37.719*AOD+1.534*Wet+3.835*Rdexp0500-0.990*Rdord0200-0.167*LCLP-0.575*PWAT+168.896	0.524	0.518	13.508	13.747	0.509	<0.0001*
	Winter	57.671*AOD+0.266*RH+2.172*Rdexp0750-0.144*LCLP-0.089*MLPT+155.119	0.570	0.564	13.223	14.453	0.516	<0.0001*
AOD-only LME model	Annual	The coefficients of random effect are seasonally varied.	0.320	0.319	15.456	16.380	0.301	<0.0001*
AOD-LUR LME model	Annual		0.375	0.374	15.755	15.797	0.374	<0.0001*
AOD-LUR GTWR models (with all included variables meet the criteria of p-value < 0.10 and VIF < 5)	Annual	The model coefficients are geographically and temporally varied. (Table S-3 - S-7 shows the coefficients of GTWR models, see the Supplementary Material).	0.542	0.541	11.598	13.523	0.461	<0.0001*
	Spring		0.617	0.615	8.590	9.693	0.536	<0.0001*
	Summer		0.899	0.898	5.885	6.254	0.839	<0.0001*
	Fall		0.709	0.708	9.071	10.460	0.606	<0.0001*
	Winter		0.640	0.639	12.120	12.158	0.634	<0.0001*

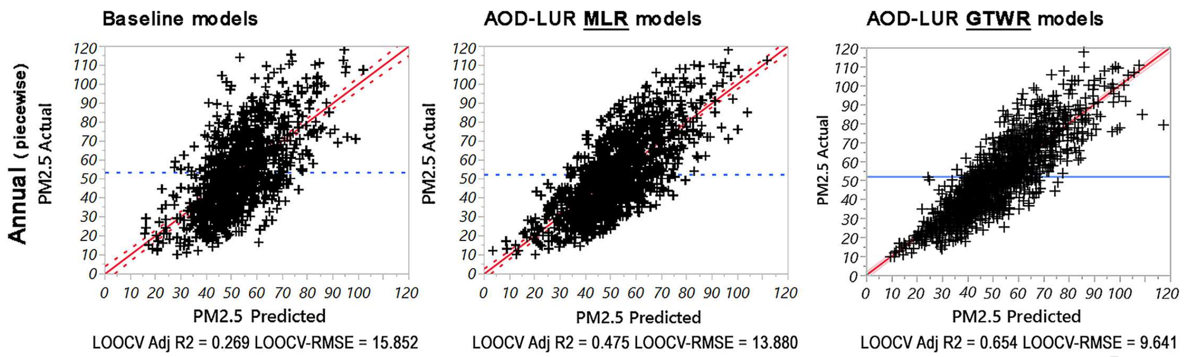

Figure 3. Actual by predicted plot of resultant piecewise models with microscale geographic predictors and sounding indices (LOOCV-$\overline{R^2}$ and LOOCV-RMSE are shown). Figure S-3 shows the results of other models.

Without forcing the structure, the resultant AOD-LUR models shows different model structures from the baseline models. First, as expected, most of the basic weather variables, instead of atmospheric sounding indices, are removed from the resultant models. A major impact factor in meteorological conditions and aerosol vertical distribution (Arya, 1999; Li et al., 2015), the atmospheric stability can be better represented by sounding indices, and consequently improve the model performance. Second, the geographic predictors of urban surface form, road traffic density and land use show in all resultant models. Traffic density and land use represent the spatial variability of the emission intensity, necessarily be the influential factors of air particle concentration in the resultant models. Under the high-density and highly heterogeneous urban context of Hong Kong, the surface forms in different areas can be considerably diverse. Urban surface forms alter the turbulent air circulation (Seinfeld, 1989), and subsequently varies the vertical profile of air particles in the boundary layer (Chan et al., 2005). Including such spatial information into the AOD-$PM_{2.5}$ correlations for LUR modelling naturally provides a better estimation of ground-level $PM_{2.5}$ variability.

3.3 AOD-LUR GEO-MAPPING

The geo-mapping of the spatial distribution of $PM_{2.5}$ was developed based on the spatiotemporal $PM_{2.5}$ estimation from the resultant AOD-LUR models. The AOD images were resampled using a cubic spline function for the mapping purpose (Bian and Xie, 2015). Seasonal average values were mapped in this paper as the right column of Figure S-3. As shown in a zoomed-in picture (Figure 4), several generally concerned air pollution hotspots, including Central, Causeway Bay in Hong Kong Island and Mong Kok, Sham Shui Po, Hung Hom in Kowloon Area can be clearly observed in the resultant geo-mapping (summer model, local-dominant air pollution mode). These areas have always been of great concerns and are commonly investigated in other local air pollution studies (Chu et al., 2005; Ho et al., 2006). Apart from the well-known air pollution hotspots, the AOD-LUR mappings developed in this paper also successfully point out another $PM_{2.5}$ hotspot, North Point on Hong Kong Island, which was newly identified by a recent study focusing on the street-level $PM_{2.5}$ exposure (Shi et al., 2016). Kok et al. (1997) already mentioned that the pollution transported from the neighboring area in Mainland China leads to poor air quality on the north and west sides of Hong Kong. In the present study, besides the local effect, a higher concentration level in the north and west part of Hong Kong can be clearly observed in the winter model (regional-dominant air pollution mode, Figure 4), which indicates that the resultant models successfully capture above situation by incorporating AOD data into LUR modelling. To be more specific, this large difference in the spatial mapping between summer and winter clearly shows the seasonal change in the dominant air pollution modes of Hong Kong. It features the local emission dominant mode in summer and the overwhelming effect of the strong regional impacts from PRD in winter (Kwok et al., 2010; Yuan et al., 2006). The above indicates that the AOD-LUR modelling in this study provides a reliable estimation of $PM_{2.5}$ for a small geographic extent in a high-density and heterogeneous urban context.

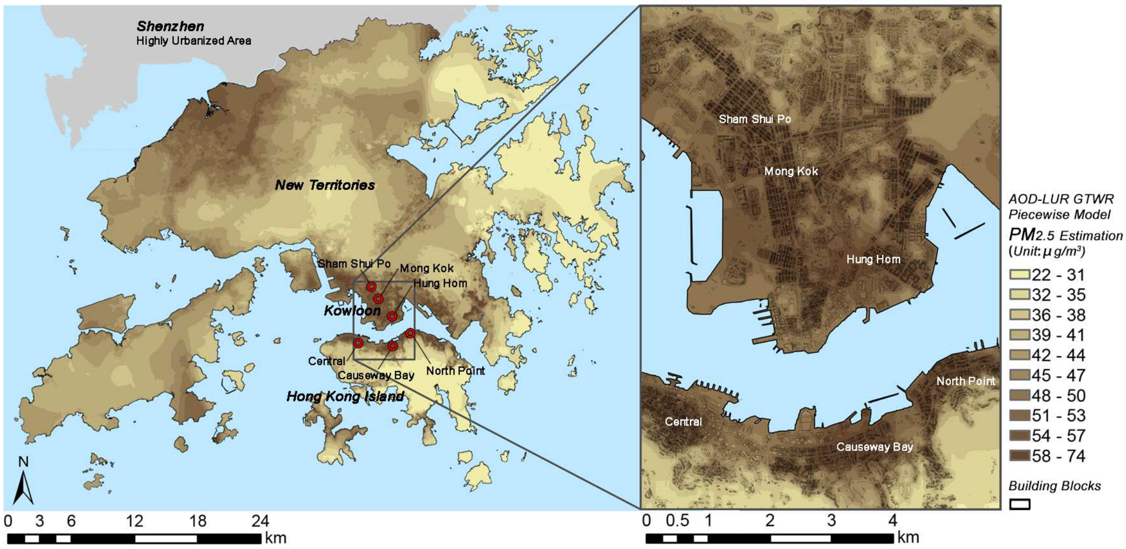

Figure 4. Resultant AOD-LUR geo-mapping with labeled $PM_{2.5}$ concentration hotspots (AOD-LUR GTWR piecewise model results).

4. DISCUSSION

4.1 IMPROVING AOD-$PM_{2.5}$ CORRELATIONS WITH MICROSCALE GEOGRAPHIC PREDICTORS AND SOUNDING INDICES

The present study improves the AOD-$PM_{2.5}$ correlation in a small geographic extent with highly heterogeneous landscapes and utilizes the result in LUR spatiotemporal $PM_{2.5}$ estimation. A previous attempt has been made for estimating the spatial variability of air particles in Hong Kong using MODIS AOD. However, the spatial scale is limited by the resolution of remote sensing images (Wong et al., 2011). Moreover, the annual average based spatial variation only provides limited information for health risk assessments without temporal estimation. In this study, the uncalibrated spatiotemporal correlation between AOD and ground-level $PM_{2.5}$ observations are substantially improved by incorporating microscale geographic predictors and atmospheric sounding indices as covariates using AOD-LUR modelling. This result makes the temporal-resolved $PM_{2.5}$ spatial estimation become viable for more accurate public health applications.

4.2 LUR MODELLING IN HIGH-DENSITY AND HETEROGENEOUS URBAN CONTEXT

On the top of the improved AOD-$PM_{2.5}$ correlations, this study also provides fine-scale mappings of $PM_{2.5}$ spatiotemporal variation based on LUR modelling. The mappings provide useful information for public health management because they help identify the $PM_{2.5}$ concentration hotspots. Identifying pollution hotspots at a fine scale is essential in Hong Kong. Under the highly heterogeneous urban context, it is impossible to identify hotspots by the sparsely distributed monitoring stations efficiently. This study shows that the monitoring gaps can be filled with remote sensing data by AOD-LUR modelling and geo-mapping techniques which are useful in the estimation of $PM_{2.5}$ human exposure level and public health applications at a finer spatial scale (Thach et al., 2015). The present study is one of the first cases of application in an extremely high-density city. Although the resultant LUR models are specially developed for Hong Kong thus cannot be entirely transferable to other locations, the present study provides a generalize-able methodology to the environment protection officers and policy-makers in other cities/regions. The way that this research analyzes the microscale urban form and integrates it into AOD-LUR modelling makes better use of the urban datasets. The analysis method could be entirely transferred and adopted to other cities. The environment protection officers and policy-makers will be able to reference it and adjusted or redevelop the prediction models based on their local settings. More importantly, the generalize-able workflow makes the prediction models and spatial estimation of different city scenarios becomes quantitatively comparable, which could contribute a more comprehensive understanding on the urban effects on air quality across different regions.

4.3 LIMITATIONS

There are a few limitations of this study, which included that the available AOD observations were directly joined to the ground-level $PM_{2.5}$ measurements. The grid cell variability in each

3 km AOD cell can only be considered on the multivariate statistical analysis stage (by using microscale geographic indices as model predictors). Future studies could be beneficial to consider the grid-cell variability of when joining AOD observations with ground-level $PM_{2.5}$ measurements.

In addition, external dataset is not available for validation in Hong Kong. With the use of only 15 ground-based monitoring stations in Hong Kong that available for model development, cross-validation was used to validate our resultant maps. This internal validation method is a strategy for validating predictions with observed data when there is lack of external data for validation (Refaeilzadeh et al., 2009), which has been widely used in previous studies for exposure mapping. Therefore, cross-validation without the use of an external dataset is appropriate for the purpose of the present study. In our next step works, attempt will be made to acquire relevant datasets from neighboring large cities (e.g. Shenzhen) for an external validation, which could also be useful to evaluate the transferability to other regions of the resultant models.

Although, the regional impact from the neighboring urbanized area in PRD region was successfully captured by our models as mentioned in section 3.3, the severe dust storm episode events due to the transport of dusts from East Asian and non-East Asian sources (Lee et al., 2010) are not well reflected in the spring models. This reveals that AOD-LUR modelling approach has a limited skill in handling the long-range transport of pollutants at a very large geographical extent. Further attempts could be made to nest the AOD-LUR models into a global or a very large regional climate/atmospheric modelling (e.g., GCMs, WRF) for geostatistical downscaling. The outputs can possibly provide a better estimation of ground-level $PM_{2.5}$ under the large-scale regional impacts.

5. CONCLUSIONS

In this study, we developed AOD-LUR spatiotemporal models of ground-level $PM_{2.5}$ concentrations and a 13-years long-term daily resolved dataset to improve the AOD-$PM_{2.5}$ correlations in a high-density city, with considerations of microscale environmental factors. On top of the AOD-$PM_{2.5}$ correlations based on the LUR model with microscale geographic predictors, we estimated the daily-resolved fine-scale spatiotemporal variation of ground-level $PM_{2.5}$ over Hong Kong. Quantitative information on the spatiotemporal variation of air pollution is essential for the planning of a densely-built urban environment because air quality is closely related to urban development. Urban development changes land cover/land use, building morphology and transportation. As a result, pollution emission increases, the local climate condition is altered and pollution dispersion is consequently affected. Compact urban development is generally regarded as a sustainable mode because it saves land resources, allows efficient use of transportation facilities. However, compact development modes without appropriate control can lead to severe urban air pollution issues (Betanzo, 2007). The AOD-LUR models developed in this study indicate that the building morphology (parameterized as the model variables of urban surface form) is actually an influential factor in air pollution concentration in a high-density urban context. Therefore, the resultant AOD-LUR models developed in this study could be potentially translated into quantitative rules and guidelines for environmental urban planning.

ACKNOWLEDGMENT

This research is supported by the General Research Fund (GRF) No.14610717 - "Developing urban planning optimization strategies for improving air quality in compact cities using geo-spatial modelling based on in-situ data" from the Research Grants Council (RGC) of Hong Kong. The authors wish to thanks the Department of Atmospheric Science, University of

Wyoming, especially Dr. Larry Oolman, for providing the atmospheric sounding indices data (Station No. 45004). The authors also would like to thank Ms. Ada Lee for her help on language. The authors appreciate reviewers for their insightful comments and constructive suggestions on our research work. The authors also want to thank editors for their patient and meticulous work for our manuscript.

REFERENCE

Arya, S.P., 1999. Air pollution meteorology and dispersion. Oxford University Press Oxford.

Babyak, M.A., 2004. What You See May Not Be What You Get: A Brief, Nontechnical Introduction to Overfitting in Regression-Type Models. Psychosom. Med. 66, 411-421.

Bach, W., 1972. Urban climate, air pollution and planning. Urbanization and environment, 69-96.

Bai, Y., Wu, L., Qin, K., Zhang, Y., Shen, Y., Zhou, Y., 2016. A Geographically and Temporally Weighted Regression Model for Ground-Level PM2.5 Estimation from Satellite-Derived 500 m Resolution AOD. Remote Sensing 8, 262.

Barnes, M.J., Brade, T.K., MacKenzie, A.R., Whyatt, J.D., Carruthers, D.J., Stocker, J., Cai, X., Hewitt, C.N., 2014. Spatially-varying surface roughness and ground-level air quality in an operational dispersion model. Environ. Pollut. 185, 44-51.

Beckerman, B.S., Jerrett, M., Serre, M., Martin, R.V., Lee, S.-J., van Donkelaar, A., Ross, Z., Su, J., Burnett, R.T., 2013. A Hybrid Approach to Estimating National Scale Spatiotemporal Variability of PM2.5 in the Contiguous United States. Environ. Sci. Technol. 47, 7233-7241.

Beelen, R., Hoek, G., Vienneau, D., Eeftens, M., Dimakopoulou, K., Pedeli, X., Tsai, M.-Y., Künzli, N., Schikowski, T., Marcon, A., 2013. Development of NO 2 and NO x land use regression models for estimating air pollution exposure in 36 study areas in Europe–the ESCAPE project. Atmos. Environ. 72, 10-23.

Betanzo, M., 2007. Pros and cons of high density urban environments. Build, April/May, 39-40.

Bian, F., Xie, Y., 2015. Geo-Informatics in Resource Management and Sustainable Ecosystem: International Conference, GRMSE 2014, Ypsilanti, USA, October 3-5, 2014, Proceedings. Springer Berlin Heidelberg.

Bilal, M., Nichol, J.E., Bleiweiss, M.P., Dubois, D., 2013. A Simplified high resolution MODIS Aerosol Retrieval Algorithm (SARA) for use over mixed surfaces. Remote Sensing of Environment 136, 135-145.

Brunsdon, C., Fotheringham, S., Charlton, M., 1998. Geographically Weighted Regression. Journal of the Royal Statistical Society: Series D (The Statistician) 47, 431-443.

Cao, M., Lin, Z., 2014. Impact of Urban Surface Roughness Length Parameterization Scheme on Urban Atmospheric Environment Simulation. Journal of Applied Mathematics 2014, 14.

Chan, C.Y., Xu, X.D., Li, Y.S., Wong, K.H., Ding, G.A., Chan, L.Y., Cheng, X.H., 2005. Characteristics of vertical profiles and sources of PM2.5, PM10 and carbonaceous species in Beijing. Atmos. Environ. 39, 5113-5124.

Cheung, H.-C., Wang, T., Baumann, K., Guo, H., 2005. Influence of regional pollution outflow on the concentrations of fine particulate matter and visibility in the coastal area of southern China. Atmos. Environ. 39, 6463-6474.

Chu, A.K.M., Kwok, R.C.W., Yu, K.N., 2005. Study of pollution dispersion in urban areas using Computational Fluid Dynamics (CFD) and Geographic Information System (GIS). Environmental Modelling & Software 20, 273-277.

Crumeyrolle, S., Chen, G., Ziemba, L., Beyersdorf, A., Thornhill, L., Winstead, E., Moore, R., Shook, M., Hudgins, C., Anderson, B., 2014. Factors that influence surface PM 2.5 values inferred from satellite observations: perspective gained for the US Baltimore–Washington metropolitan area during DISCOVER-AQ. Atmospheric Chemistry and Physics 14, 2139-2153.

Davidson, C.I., Phalen, R.F., Solomon, P.A., 2005. Airborne Particulate Matter and Human Health: A Review. Aerosol Sci. Technol. 39, 737-749.

de Hoogh, K., Gulliver, J., Donkelaar, A.v., Martin, R.V., Marshall, J.D., Bechle, M.J., Cesaroni, G., Pradas, M.C., Dedele, A., Eeftens, M., Forsberg, B., Galassi, C., Heinrich, J., Hoffmann, B., Jacquemin, B., Katsouyanni, K., Korek, M., Künzli, N., Lindley, S.J., Lepeule, J., Meleux, F., de Nazelle, A., Nieuwenhuijsen, M., Nystad, W., Raaschou-Nielsen, O., Peters, A., Peuch, V.-H., Rouil, L., Udvardy, O., Slama, R., Stempfelet, M., Stephanou, E.G., Tsai, M.Y., Yli-Tuomi, T., Weinmayr, G., Brunekreef, B., Vienneau, D., Hoek, G., 2016. Development of West-European PM2.5 and NO2 land use regression models incorporating satellite-derived and chemical transport modelling data. Environ. Res. 151, 1-10.

Ding, A., Wang, T., Fu, C., 2013. Transport characteristics and origins of carbon monoxide and ozone in Hong Kong, South China. Journal of Geophysical Research: Atmospheres 118, 9475-9488.

Dockery, D.W., 2009. Health Effects of Particulate Air Pollution. Annals of Epidemiology 19, 257-263.

EPA, 2013. Particulate Matter (PM). United States Environmental Protection Agency.

Fernando, H.J.S., Lee, S.M., Anderson, J., Princevac, M., Pardyjak, E., Grossman-Clarke, S., 2001. Urban Fluid Mechanics: Air Circulation and Contaminant Dispersion in Cities. Environmental Fluid Mechanics 1, 107-164.

Geng, G., Zhang, Q., Martin, R.V., van Donkelaar, A., Huo, H., Che, H., Lin, J., He, K., 2015. Estimating long-term PM2.5 concentrations in China using satellite-based aerosol optical depth and a chemical transport model. Remote Sensing of Environment 166, 262-270.

Ho, H.C., Knudby, A., Sirovyak, P., Xu, Y., Hodul, M., Henderson, S.B., 2014. Mapping maximum urban air temperature on hot summer days. Remote Sensing of Environment 154, 38-45.

Ho, K.F., Cao, J.J., Lee, S.C., Chan, C.K., 2006. Source apportionment of PM 2.5 in urban area of Hong Kong. J. Hazard. Mater. 138, 73-85.

Hoek, G., Beelen, R., de Hoogh, K., Vienneau, D., Gulliver, J., Fischer, P., Briggs, D., 2008. A review of land-use regression models to assess spatial variation of outdoor air pollution. Atmos. Environ. 42, 7561-7578.

Hoff, R.M., Christopher, S.A., 2009. Remote Sensing of Particulate Pollution from Space: Have We Reached the Promised Land? Journal of the Air & Waste Management Association 59, 645-675.

Huang, B., Wu, B., Barry, M., 2010. Geographically and temporally weighted regression for modeling spatio-temporal variation in house prices. International Journal of Geographical Information Science 24, 383-401.

Jonsson, P., Bennet, C., Eliasson, I., Selin Lindgren, E., 2004. Suspended particulate matter and its relations to the urban climate in Dar es Salaam, Tanzania. Atmos. Environ. 38, 4175-4181.

Kanaroglou, P.S., Jerrett, M., Morrison, J., Beckerman, B., Arain, M.A., Gilbert, N.L., Brook, J.R., 2005. Establishing an air pollution monitoring network for intra-urban population exposure assessment: A location-allocation approach. Atmos. Environ. 39, 2399-2409.

Kloog, I., Nordio, F., Coull, B.A., Schwartz, J., 2012. Incorporating Local Land Use Regression And Satellite Aerosol Optical Depth In A Hybrid Model Of Spatiotemporal PM2.5 Exposures In The Mid-Atlantic States. Environ. Sci. Technol. 46, 11913-11921.

Kok, G.L., Lind, J.A., Fang, M., 1997. An airborne study of air quality around the Hong Kong territory. Journal of Geophysical Research: Atmospheres 102, 19043-19057.

Krstic, N., Henderson, S.B., 2015. Use of MODIS data to assess atmospheric aerosol before, during, and after community evacuations related to wildfire smoke. Remote Sensing of Environment 166, 1-7.

Kwok, R.H., Fung, J.C., Lau, A.K., Fu, J.S., 2010. Numerical study on seasonal variations of gaseous pollutants and particulate matters in Hong Kong and Pearl River Delta Region. Journal of Geophysical Research: Atmospheres (1984–2012) 115.

Lau, A., Lo, A., Gray, J., Yuan, Z., Loh, C., 2007. Relative significance of local vs. regional sources: Hong Kong's air pollution. Civic Exchange.

Lee, H., Liu, Y., Coull, B., Schwartz, J., Koutrakis, P., 2011. A novel calibration approach of MODIS AOD data to predict PM2. 5 concentrations. Atmos. Chem. Phys 11, 7991-8002.

Lee, H.J., Chatfield, R.B., Strawa, A.W., 2016. Enhancing the Applicability of Satellite Remote Sensing for PM2.5 Estimation Using MODIS Deep Blue AOD and Land Use Regression in California, United States. Environ. Sci. Technol. 50, 6546-6555.

Lee, Y.C., Yang, X., Wenig, M., 2010. Transport of dusts from East Asian and non-East Asian sources to Hong Kong during dust storm related events 1996–2007. Atmos. Environ. 44, 3728-3738.

Li, J., Carlson, B.E., Lacis, A.A., 2015. How well do satellite AOD observations represent the spatial and temporal variability of PM2.5 concentration for the United States? Atmos. Environ. 102, 260-273.

Lin, H., Ma, W., Qiu, H., Wang, X., Trevathan, E., Yao, Z., Dong, G.-H., Vaughn, M.G., Qian, Z., Tian, L., 2017. Using daily excessive concentration hours to explore the short-term mortality effects of ambient PM2. 5 in Hong Kong. Environ. Pollut. 229, 896-901.

Liu, Y., Park, R.J., Jacob, D.J., Li, Q., Kilaru, V., Sarnat, J.A., 2004. Mapping annual mean ground-level PM2.5 concentrations using Multiangle Imaging Spectroradiometer aerosol optical thickness over the contiguous United States. Journal of Geophysical Research: Atmospheres 109, n/a-n/a.

Lu, W.-Z., Wang, X.-K., 2008. Investigation of respirable suspended particulate trend and relevant environmental factors in Hong Kong downtown areas. Chemosphere 71, 561-567.

Mao, L., Qiu, Y., Kusano, C., Xu, X., 2012. Predicting regional space–time variation of PM2.5 with land-use regression model and MODIS data. Environ Sci Pollut Res 19, 128-138.

Paciorek, C.J., Liu, Y., Moreno-Macias, H., Kondragunta, S., 2008. Spatiotemporal Associations between GOES Aerosol Optical Depth Retrievals and Ground-Level PM2.5. Environ. Sci. Technol. 42, 5800-5806.

Pope, C.A., Dockery, D.W., Schwartz, J., 1995. Review of epidemiological evidence of health effects of particulate air pollution. Inhalation Toxicol. 7, 1-18.

Qin, K., Wang, L., Wu, L., Xu, J., Rao, L., Letu, H., Shi, T., Wang, R., 2017. A campaign for investigating aerosol optical properties during winter hazes over Shijiazhuang, China. Atmospheric Research 198, 113-122.

Refaeilzadeh, P., Tang, L., Liu, H., 2009. Cross-Validation, in: Liu, L., ÖZsu, M.T. (Eds.), Encyclopedia of Database Systems. Springer US, Boston, MA, pp. 532-538.

Remer, L.A., Mattoo, S., Levy, R.C., Munchak, L.A., 2013. MODIS 3 km aerosol product: algorithm and global perspective. Atmos. Meas. Tech. 6, 1829-1844.

Ryan, P.H., LeMasters, G.K., 2007. A review of land-use regression models for characterizing intraurban air pollution exposure. Inhalation Toxicol. 19, 127-133.

Saraswat, A., Apte, J.S., Kandlikar, M., Brauer, M., Henderson, S.B., Marshall, J.D., 2013. Spatiotemporal Land Use Regression Models of Fine, Ultrafine, and Black Carbon Particulate Matter in New Delhi, India. Environ. Sci. Technol. 47, 12903-12911.

Schwarze, P.E., Øvrevik, J., Låg, M., Refsnes, M., Nafstad, P., Hetland, R.B., Dybing, E., 2006. Particulate matter properties and health effects: consistency of epidemiological and toxicological studies. Human & Experimental Toxicology 25, 559-579.

Seinfeld, J.H., 1989. Urban Air Pollution: State of the Science. Science 243, 745.

Shi, Y., Lau, K.K.-L., Ng, E., 2016. Developing Street-Level PM2.5 and PM10 Land Use Regression Models in High-Density Hong Kong with Urban Morphological Factors. Environ. Sci. Technol. 50, 8178-8187.

Shi, Y., Lau, K.K.-L., Ng, E., 2017. Incorporating wind availability into land use regression modelling of air quality in mountainous high-density urban environment. Environ. Res. 157, 17-29.

Su, J.G., Jerrett, M., Beckerman, B., 2009a. A distance-decay variable selection strategy for land use regression modeling of ambient air pollution exposures. Sci. Total Environ. 407, 3890-3898.

Su, J.G., Jerrett, M., Beckerman, B., Wilhelm, M., Ghosh, J.K., Ritz, B., 2009b. Predicting traffic-related air pollution in Los Angeles using a distance decay regression selection strategy. Environ. Res. 109, 657-670.

Tam, W.W.S., Wong, T.W., Wong, A.H.S., 2015. Association between air pollution and daily mortality and hospital admission due to ischaemic heart diseases in Hong Kong. Atmos. Environ. 120, 360-368.

Tang, R., Blangiardo, M., Gulliver, J., 2013. Using Building Heights and Street Configuration to Enhance Intraurban PM10, NOX, and NO2 Land Use Regression Models. Environ. Sci. Technol. 47, 11643-11650.

Thach, T.-Q., Wong, C.-M., Chan, K.-P., Chau, Y.-K., Chung, Y.-N., Ou, C.-Q., Yang, L., Hedley, A.J., 2010. Daily visibility and mortality: Assessment of health benefits from improved visibility in Hong Kong. Environ. Res. 110, 617-623.

Thach, T.-Q., Zheng, Q., Lai, P.-C., Wong, P.P.-Y., Chau, P.Y.-K., Jahn, H.J., Plass, D., Katzschner, L., Kraemer, A., Wong, C.-M., 2015. Assessing spatial associations between thermal stress and mortality in Hong Kong: A small-area ecological study. Sci. Total Environ. 502, 666-672.

van Donkelaar, A., Martin, R.V., Park, R.J., 2006. Estimating ground-level PM2.5 using aerosol optical depth determined from satellite remote sensing. Journal of Geophysical Research: Atmospheres 111, n/a-n/a.

van Donkelaar, A., Martin, R.V., Spurr, R.J.D., Burnett, R.T., 2015. High-Resolution Satellite-Derived PM2.5 from Optimal Estimation and Geographically Weighted Regression over North America. Environ. Sci. Technol. 49, 10482-10491.

Vienneau, D., de Hoogh, K., Bechle, M.J., Beelen, R., van Donkelaar, A., Martin, R.V., Millet, D.B., Hoek, G., Marshall, J.D., 2013. Western European Land Use Regression Incorporating Satellite- and Ground-Based Measurements of NO2 and PM10. Environ. Sci. Technol. 47, 13555-13564.

Wang, T., Wei, X.L., Ding, A.J., Poon, C.N., Lam, K.S., Li, Y.S., Chan, L.Y., Anson, M., 2009. Increasing surface ozone concentrations in the background atmosphere of Southern China, 1994–2007. Atmos. Chem. Phys. 9, 6217-6227.

Wang, X.-K., Lu, W.-Z., 2006. Seasonal variation of air pollution index: Hong Kong case study. Chemosphere 63, 1261-1272.

Wong, M.S., Nichol, J., Lee, K.H., Lee, B.Y., 2011. Monitoring 2.5 μm particulate matter within urbanized regions using satellite-derived aerosol optical thickness, a study in Hong Kong. International Journal of Remote Sensing 32, 8449-8462.

Wong, T.W., Lau, T.S., Yu, T.S., Neller, A., Wong, S.L., Tam, W., Pang, S.W., 1999. Air pollution and hospital admissions for respiratory and cardiovascular diseases in Hong Kong. Occupational and Environmental Medicine 56, 679-683.

Wong, T.W., Tam, W.S., Yu, T.S., Wong, A.H.S., 2002. Associations between daily mortalities from respiratory and cardiovascular diseases and air pollution in Hong Kong, China. Occupational and Environmental Medicine 59, 30-35.

Wu, D., Tie, X., Li, C., Ying, Z., Kai-Hon Lau, A., Huang, J., Deng, X., Bi, X., 2005. An extremely low visibility event over the Guangzhou region: A case study. Atmos. Environ. 39, 6568-6577.

Xie, Y., Wang, Y., Zhang, K., Dong, W., Lv, B., Bai, Y., 2015. Daily Estimation of Ground-Level PM2.5 Concentrations over Beijing Using 3 km Resolution MODIS AOD. Environ. Sci. Technol. 49, 12280-12288.

You, W., Zang, Z., Zhang, L., Li, Y., Pan, X., Wang, W., 2016. National-Scale Estimates of Ground-Level PM2.5 Concentration in China Using Geographically Weighted Regression Based on 3 km Resolution MODIS AOD. Remote Sensing 8, 184.

Yuan, C., Ng, E., Norford, L.K., 2014. Improving air quality in high-density cities by understanding the relationship between air pollutant dispersion and urban morphologies. Build Environ. 71, 245-258.

Yuan, Z., Lau, A.K.H., Zhang, H., Yu, J.Z., Louie, P.K.K., Fung, J.C.H., 2006. Identification and spatiotemporal variations of dominant PM10 sources over Hong Kong. Atmos. Environ. 40, 1803-1815.

Zang, Z., Wang, W., You, W., Li, Y., Ye, F., Wang, C., 2017. Estimating ground-level PM2.5 concentrations in Beijing, China using aerosol optical depth and parameters of the temperature inversion layer. Sci. Total Environ. 575, 1219-1227.

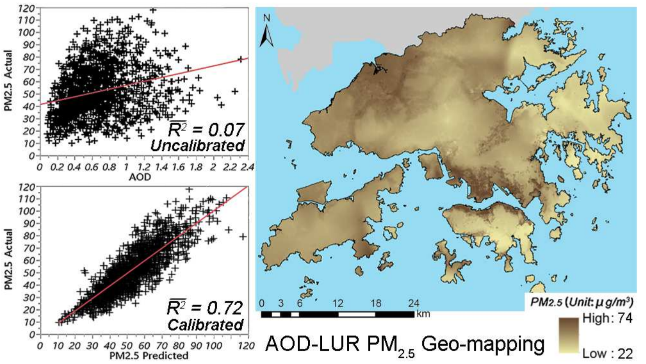

PM2.5 Actual
AOD
$\overline{R}^2$ = 0.07
Uncalibrated
PM2.5 Actual
PM2.5 Predicted
$\overline{R}^2$ = 0.72
Calibrated
N
0 3 6 12 18 24 km
PM2.5 (Unit: μg/m³)
High: 74
Low : 22
AOD-LUR PM2.5 Geo-mapping